Observation of pseudoscalar and tensor resonances in $J/\psi \to \gamma\phi\phi$

M. Ablikim,[1] M. N. Achasov,[9,e] X. C. Ai,[1] O. Albayrak,[5] M. Albrecht,[4] D. J. Ambrose,[44] A. Amoroso,[49a,49c] F. F. An,[1] Q. An,[46,*] J. Z. Bai,[1] R. Baldini Ferroli,[20a] Y. Ban,[31] D. W. Bennett,[19] J. V. Bennett,[5] M. Bertani,[20a] D. Bettoni,[21a] J. M. Bian,[43] F. Bianchi,[49a,49c] E. Boger,[23,‡] I. Boyko,[23] R. A. Briere,[5] H. Cai,[51] X. Cai,[1,*] O. Cakir,[40a] A. Calcaterra,[20a] G. F. Cao,[1] S. A. Cetin,[40b] J. F. Chang,[1,*] G. Chelkov,[23,‡,§] G. Chen,[1] H. S. Chen,[1] H. Y. Chen,[2] J. C. Chen,[1] M. L. Chen,[1,*] S. J. Chen,[29] X. Chen,[1,*] X. R. Chen,[26] Y. B. Chen,[1,*] H. P. Cheng,[17] X. K. Chu,[31] G. Cibinetto,[21a] H. L. Dai,[1,*] J. P. Dai,[34] A. Dbeyssi,[14] D. Dedovich,[23] Z. Y. Deng,[1] A. Denig,[22] I. Denysenko,[23] M. Destefanis,[49a,49c] F. De Mori,[49a,49c] Y. Ding,[27] C. Dong,[30] J. Dong,[1,*] L. Y. Dong,[1] M. Y. Dong,[1,*] Z. L. Dou,[29] S. X. Du,[53] P. F. Duan,[1] J. Z. Fan,[39] J. Fang,[1,*] S. S. Fang,[1] X. Fang,[46,*] Y. Fang,[1] R. Farinelli,[21a,21b] L. Fava,[49b,49c] O. Fedorov,[23] F. Feldbauer,[22] G. Felici,[20a] C. Q. Feng,[46,*] E. Fioravanti,[21a] M. Fritsch,[14,22] C. D. Fu,[1] Q. Gao,[1] X. L. Gao,[46,*] X. Y. Gao,[2] Y. Gao,[39] Z. Gao,[46,*] I. Garzia,[21a] K. Goetzen,[10] L. Gong,[30] W. X. Gong,[1,*] W. Gradl,[22] M. Greco,[49a,49c] M. H. Gu,[1,*] Y. T. Gu,[12] Y. H. Guan,[1] A. Q. Guo,[1] L. B. Guo,[28] Y. Guo,[1] Y. P. Guo,[22] Z. Haddadi,[25] A. Hafner,[22] S. Han,[51] X. Q. Hao,[15] F. A. Harris,[42] K. L. He,[1] T. Held,[4] Y. K. Heng,[1,*] Z. L. Hou,[1] C. Hu,[28] H. M. Hu,[1] J. F. Hu,[49a,49c] T. Hu,[1,*] Y. Hu,[1] G. S. Huang,[46,*] J. S. Huang,[15] X. T. Huang,[33] Y. Huang,[29] T. Hussain,[48] Q. Ji,[1] Q. P. Ji,[30] X. B. Ji,[1] X. L. Ji,[1,*] L. W. Jiang,[51] X. S. Jiang,[1,*] X. Y. Jiang,[30] J. B. Jiao,[33] Z. Jiao,[17] D. P. Jin,[1,*] S. Jin,[1] T. Johansson,[50] A. Julin,[43] N. Kalantar-Nayestanaki,[25] X. L. Kang,[1] X. S. Kang,[30] M. Kavatsyuk,[25] B. C. Ke,[5] P. Kiese,[22] R. Kliemt,[14] B. Kloss,[22] O. B. Kolcu,[40b,††] B. Kopf,[4] M. Kornicer,[42] A. Kupsc,[50] W. Kühn,[24] J. S. Lange,[24] M. Lara,[19] P. Larin,[14] C. Leng,[40c] C. Li,[50] Cheng Li,[46,*] D. M. Li,[53] F. Li,[1,*] F. Y. Li,[31] G. Li,[1] H. B. Li,[1] J. C. Li,[1] Jin Li,[32] K. Li,[33] K. Li,[13] Lei Li,[3] P. R. Li,[41] Q. Y. Li,[33] T. Li,[33] W. D. Li,[1] W. G. Li,[1] X. L. Li,[33] X. N. Li,[1,*] X. Q. Li,[30] Z. B. Li,[38] H. Liang,[46,*] Y. F. Liang,[36] Y. T. Liang,[24] G. R. Liao,[11] D. X. Lin,[14] B. J. Liu,[1] C. X. Liu,[1] D. Liu,[46,*] F. H. Liu,[35] Fang Liu,[1] Feng Liu,[6] H. B. Liu,[12] H. H. Liu,[16] H. H. Liu,[1] H. M. Liu,[1] J. Liu,[1] J. B. Liu,[46,*] J. P. Liu,[51] J. Y. Liu,[1] K. Liu,[39] K. Y. Liu,[27] L. D. Liu,[31] P. L. Liu,[1,*] Q. Liu,[41] S. B. Liu,[46,*] X. Liu,[26] Y. B. Liu,[30] Z. A. Liu,[1,*] Zhiqing Liu,[22] H. Loehner,[25] X. C. Lou,[1,*,**;] H. J. Lu,[17] J. G. Lu,[1,*] Y. Lu,[1] Y. P. Lu,[1,*] C. L. Luo,[28] M. X. Luo,[52] T. Luo,[42] X. L. Luo,[1,*] X. R. Lyu,[41] F. C. Ma,[27] H. L. Ma,[1] L. L. Ma,[33] Q. M. Ma,[1] T. Ma,[1] X. N. Ma,[30] X. Y. Ma,[1,*] Y. M. Ma,[33] F. E. Maas,[14] M. Maggiora,[49a,49c] Y. J. Mao,[31] Z. P. Mao,[1] S. Marcello,[49a,49c] J. G. Messchendorp,[25] J. Min,[1,*] R. E. Mitchell,[19] X. H. Mo,[1,*] Y. J. Mo,[6] C. Morales Morales,[14] N. Yu. Muchnoi,[9,e] H. Muramatsu,[43] Y. Nefedov,[23] F. Nerling,[14] I. B. Nikolaev,[9,e] Z. Ning,[1,*] S. Nisar,[8] S. L. Niu,[1,*] X. Y. Niu,[1] S. L. Olsen,[32] Q. Ouyang,[1,*] S. Pacetti,[20b] Y. Pan,[46,*] P. Patteri,[20a] M. Pelizaeus,[4] H. P. Peng,[46,*] K. Peters,[10] J. Pettersson,[50] J. L. Ping,[28] R. G. Ping,[1] R. Poling,[43] V. Prasad,[1] H. R. Qi,[2] M. Qi,[29] S. Qian,[1,*] C. F. Qiao,[41] L. Q. Qin,[33] N. Qin,[51] X. S. Qin,[1] Z. H. Qin,[1,*] J. F. Qiu,[1] K. H. Rashid,[48] C. F. Redmer,[22] M. Ripka,[22] G. Rong,[1] Ch. Rosner,[14] X. D. Ruan,[12] V. Santoro,[21a] A. Sarantsev,[23,¶] M. Savrié,[21b] K. Schoenning,[50] S. Schumann,[22] W. Shan,[31] M. Shao,[46,*] C. P. Shen,[2] P. X. Shen,[30] X. Y. Shen,[1] H. Y. Sheng,[1] W. M. Song,[1] X. Y. Song,[1] S. Sosio,[49a,49c] S. Spataro,[49a,49c] G. X. Sun,[1] J. F. Sun,[15] S. S. Sun,[1] Y. J. Sun,[46,*] Y. Z. Sun,[1] Z. J. Sun,[1,*] Z. T. Sun,[19] C. J. Tang,[36] X. Tang,[1] I. Tapan,[40c] E. H. Thorndike,[44] M. Tiemens,[25] M. Ullrich,[24] I. Uman,[40d] G. S. Varner,[42] B. Wang,[30] B. L. Wang,[41] D. Wang,[31] D. Y. Wang,[31] K. Wang,[1,*] L. L. Wang,[1] L. S. Wang,[1] M. Wang,[33] P. Wang,[1] P. L. Wang,[1] S. G. Wang,[31] W. Wang,[1,*] W. P. Wang,[46,*] X. F. Wang,[39] Y. D. Wang,[14] Y. F. Wang,[1,*] Y. Q. Wang,[22] Z. Wang,[1,*] Z. G. Wang,[1,*] Z. H. Wang,[46,*] Z. Y. Wang,[1] T. Weber,[22] D. H. Wei,[11] J. B. Wei,[31] P. Weidenkaff,[22] S. P. Wen,[1] U. Wiedner,[4] M. Wolke,[50] L. H. Wu,[1] Z. Wu,[1,*] L. Xia,[46,*] L. G. Xia,[39] Y. Xia,[18] D. Xiao,[1] H. Xiao,[47] Z. J. Xiao,[28] Y. G. Xie,[1,*] Q. L. Xiu,[1,*] G. F. Xu,[1] L. Xu,[1] Q. J. Xu,[13] Q. N. Xu,[41] X. P. Xu,[37] L. Yan,[49a,49c] W. B. Yan,[46,*] W. C. Yan,[46,*] Y. H. Yan,[18] H. J. Yang,[34] H. X. Yang,[1] L. Yang,[51] Y. X. Yang,[11] M. Ye,[1,*] M. H. Ye,[7] J. H. Yin,[1] B. X. Yu,[1,*] C. X. Yu,[30] J. S. Yu,[26] C. Z. Yuan,[1] W. L. Yuan,[29] Y. Yuan,[1] A. Yuncu,[40b,†] A. A. Zafar,[48] A. Zallo,[20a] Y. Zeng,[18] Z. Zeng,[46,*] B. X. Zhang,[1] B. Y. Zhang,[1,*] C. Zhang,[29] C. C. Zhang,[1] D. H. Zhang,[1] H. H. Zhang,[38] H. Y. Zhang,[1,*] J. J. Zhang,[1] J. L. Zhang,[1] J. Q. Zhang,[1] J. W. Zhang,[1,*] J. Y. Zhang,[1] J. Z. Zhang,[1] K. Zhang,[1] L. Zhang,[1] X. Y. Zhang,[33] Y. Zhang,[1] Y. H. Zhang,[1,*] Y. N. Zhang,[41] Y. T. Zhang,[46,*] Yu Zhang,[41] Z. H. Zhang,[6] Z. P. Zhang,[46] Z. Y. Zhang,[51] G. Zhao,[1] J. W. Zhao,[1,*] J. Y. Zhao,[1] J. Z. Zhao,[1,*] Lei Zhao,[46,*] Ling Zhao,[1] M. G. Zhao,[30] Q. Zhao,[1] Q. W. Zhao,[1] S. J. Zhao,[53] T. C. Zhao,[1] Y. B. Zhao,[1,*] Z. G. Zhao,[46,*] A. Zhemchugov,[23,‡] B. Zheng,[47] J. P. Zheng,[1,*] W. J. Zheng,[33] Y. H. Zheng,[41] B. Zhong,[28] L. Zhou,[1,*] X. Zhou,[51] X. K. Zhou,[46,*] X. R. Zhou,[46,*] X. Y. Zhou,[1] K. Zhu,[1] K. J. Zhu,[1,*] S. Zhu,[1] S. H. Zhu,[45] X. L. Zhu,[39] Y. C. Zhu,[46,*] Y. S. Zhu,[1] Z. A. Zhu,[1] J. Zhuang,[1,*] L. Zotti,[49a,49c] B. S. Zou,[1] and J. H. Zou[1]

(BESIII Collaboration)

[1]*Institute of High Energy Physics, Beijing 100049, People's Republic of China*
[2]*Beihang University, Beijing 100191, People's Republic of China*
[3]*Beijing Institute of Petrochemical Technology, Beijing 102617, People's Republic of China*
[4]*Bochum Ruhr-University, D-44780 Bochum, Germany*
[5]*Carnegie Mellon University, Pittsburgh, Pennsylvania 15213, USA*

[6]*Central China Normal University, Wuhan 430079, People's Republic of China*
[7]*China Center of Advanced Science and Technology, Beijing 100190, People's Republic of China*
[8]*COMSATS Institute of Information Technology, Lahore, Defence Road, Off Raiwind Road, 54000 Lahore, Pakistan*
[9]*G.I. Budker Institute of Nuclear Physics SB RAS (BINP), Novosibirsk 630090, Russia*
[10]*GSI Helmholtzcentre for Heavy Ion Research GmbH, D-64291 Darmstadt, Germany*
[11]*Guangxi Normal University, Guilin 541004, People's Republic of China*
[12]*GuangXi University, Nanning 530004, People's Republic of China*
[13]*Hangzhou Normal University, Hangzhou 310036, People's Republic of China*
[14]*Helmholtz Institute Mainz, Johann-Joachim-Becher-Weg 45, D-55099 Mainz, Germany*
[15]*Henan Normal University, Xinxiang 453007, People's Republic of China*
[16]*Henan University of Science and Technology, Luoyang 471003, People's Republic of China*
[17]*Huangshan College, Huangshan 245000, People's Republic of China*
[18]*Hunan University, Changsha 410082, People's Republic of China*
[19]*Indiana University, Bloomington, Indiana 47405, USA*
[20a]*INFN Laboratori Nazionali di Frascati, I-00044, Frascati, Italy*
[20b]*INFN and University of Perugia, I-06100 Perugia, Italy*
[21a]*INFN Sezione di Ferrara, I-44122 Ferrara, Italy*
[21b]*University of Ferrara, I-44122 Ferrara, Italy*
[22]*Johannes Gutenberg University of Mainz, Johann-Joachim-Becher-Weg 45, D-55099 Mainz, Germany*
[23]*Joint Institute for Nuclear Research, 141980 Dubna, Moscow region, Russia*
[24]*Justus-Liebig-Universitaet Giessen, II. Physikalisches Institut, Heinrich-Buff-Ring 16, D-35392 Giessen, Germany*
[25]*KVI-CART, University of Groningen, NL-9747 AA Groningen, The Netherlands*
[26]*Lanzhou University, Lanzhou 730000, People's Republic of China*
[27]*Liaoning University, Shenyang 110036, People's Republic of China*
[28]*Nanjing Normal University, Nanjing 210023, People's Republic of China*
[29]*Nanjing University, Nanjing 210093, People's Republic of China*
[30]*Nankai University, Tianjin 300071, People's Republic of China*
[31]*Peking University, Beijing 100871, People's Republic of China*
[32]*Seoul National University, Seoul 151-747, Korea*
[33]*Shandong University, Jinan 250100, People's Republic of China*
[34]*Shanghai Jiao Tong University, Shanghai 200240, People's Republic of China*
[35]*Shanxi University, Taiyuan 030006, People's Republic of China*
[36]*Sichuan University, Chengdu 610064, People's Republic of China*
[37]*Soochow University, Suzhou 215006, People's Republic of China*
[38]*Sun Yat-Sen University, Guangzhou 510275, People's Republic of China*
[39]*Tsinghua University, Beijing 100084, People's Republic of China*
[40a]*Ankara University, 06100 Tandogan, Ankara, Turkey*
[40b]*Istanbul Bilgi University, 34060 Eyup, Istanbul, Turkey*
[40c]*Uludag University, 16059 Bursa, Turkey*
[40d]*Near East University, Nicosia, North Cyprus, Mersin 10, Turkey*
[41]*University of Chinese Academy of Sciences, Beijing 100049, People's Republic of China*
[42]*University of Hawaii, Honolulu, Hawaii 96822, USA*
[43]*University of Minnesota, Minneapolis, Minnesota 55455, USA*
[44]*University of Rochester, Rochester, New York 14627, USA*
[45]*University of Science and Technology Liaoning, Anshan 114051, People's Republic of China*
[46]*University of Science and Technology of China, Hefei 230026, People's Republic of China*
[47]*University of South China, Hengyang 421001, People's Republic of China*
[48]*University of the Punjab, Lahore 54590, Pakistan*
[49a]*University of Turin, I-10125 Turin, Italy*
[49b]*University of Eastern Piedmont, I-15121 Alessandria, Italy*
[49c]*INFN, I-10125 Turin, Italy*

[50]Uppsala University, Box 516, SE-75120 Uppsala, Sweden
[51]Wuhan University, Wuhan 430072, People's Republic of China
[52]Zhejiang University, Hangzhou 310027, People's Republic of China
[53]Zhengzhou University, Zhengzhou 450001, People's Republic of China
(Received 5 February 2016; published 20 June 2016)

Based on a sample of $(1310.6 \pm 10.5) \times 10^6$ J/ψ events collected with the BESIII detector operating at the BEPCII storage ring, a partial wave analysis of the decay $J/\psi \to \gamma\phi\phi$ is performed in order to study the intermediate states. Results of the partial wave analysis show that the structures are predominantly 0^{-+} states. The existence of the $\eta(2225)$ is confirmed, and its resonance parameters are measured. Two additional pseudoscalar states, the $\eta(2100)$ with a mass of 2050^{+30+75}_{-24-26} MeV/c^2 and a width of $250^{+36+181}_{-30-164}$ MeV/c^2 and the $X(2500)$ with a mass of $2470^{+15+101}_{-19-23}$ MeV/c^2 and a width of 230^{+64+56}_{-35-33} MeV/c^2, are observed. In addition to these three pseudoscalar states, the scalar state $f_0(2100)$, and three tensor states, the $f_2(2010)$, $f_2(2300)$ and $f_2(2340)$, are observed in the process $J/\psi \to \gamma\phi\phi$. The product branching fractions $\mathcal{B}(J/\psi \to \gamma X) \times \mathcal{B}(X \to \phi\phi)$ are reported.

DOI: 10.1103/PhysRevD.93.112011

I. INTRODUCTION

In quantum chromodynamics (QCD), gluons—the gauge bosons of the strong force—carry color charge and thus can form bound states called glueballs [1–3]. The search for glueballs is an important field of research in hadron physics. However, possible mixing of the pure glueball states with nearby $q\bar{q}$ nonet mesons makes the identification of glueballs difficult in both experiment and theory. The glueball spectrum has been predicted by Lattice QCD [4–6], where the lowest-lying glueballs are scalar (mass 1.5–1.7 GeV/c^2), tensor (mass 2.3–2.4 GeV/c^2), and pseudoscalar (mass 2.3–2.6 GeV/c^2). Radiative decays of the J/ψ meson provide a gluon-rich environment and are, therefore, regarded as one of the most promising hunting grounds for glueballs [7,8].

Broad $J^{PC} = 2^{++}$ structures around 2.3 GeV/c^2 decaying to $\phi\phi$ were reported in $\pi^- N$ reactions [9,10] and in $p\bar{p}$ central collisions [11,12]. In Ref. [13,14], a tensor glueball was assumed to be mixed with conventional tensor resonances. Aside from the $\eta(2225)$, which was discovered in $J/\psi \to \gamma\phi\phi$ [15–17], the structures in the pseudoscalar sector above 2 GeV/c^2 are poorly understood.

In this paper, we present a partial wave analysis (PWA) of $J/\psi \to \gamma\phi\phi$, where both ϕ mesons are reconstructed from K^+K^-, based on a sample of $(1310.6 \pm 10.5) \times 10^6$ J/ψ events collected with the BESIII detector [18].

II. BESIII DETECTOR AND MONTE CARLO SIMULATION

The BESIII detector is a magnetic spectrometer operating at BEPCII, a double-ring e^+e^- collider with center-of-mass energies between 2.0 and 4.6 GeV. The cylindrical core of the BESIII detector consists of a helium-based main drift chamber (MDC), a plastic scintillator time-of-flight system (TOF) and a CsI(Tl) electromagnetic calorimeter (EMC) that are all enclosed in a superconducting solenoidal magnet providing a magnetic field of 1.0 T (0.9 T in 2012, for about 1.09×10^9 J/ψ events). The solenoid is supported by an octagonal flux-return yoke with resistive plate counter muon identifier modules interleaved with steel. The acceptance for charged particles and photons is 93% of the 4π solid angle, and the charged-particle momentum resolution at $p = 1$ GeV/c is 0.5%. The EMC measures photon energies with a resolution of 2.5% (5%) at $E_\gamma = 1$ GeV in the barrel (end caps).

A GEANT4-based [19] Monte Carlo (MC) simulation software package is used to optimize the event selection criteria, estimate backgrounds and determine the detection efficiency. We generate a large signal MC sample of $J/\psi \to \gamma\phi\phi$, $\phi \to K^+K^-$ uniformly in phase space.

III. EVENT SELECTION

Charged tracks in the polar angle range $|\cos\theta| < 0.93$ are reconstructed from hits in the MDC. The combined information from the energy loss (dE/dx) measured in

*Also at the Novosibirsk State University, Novosibirsk, 630090, Russia.
†Also at State Key Laboratory of Particle Detection and Electronics, Beijing 100049, Hefei 230026, People's Republic of China.
‡Also at the Moscow Institute of Physics and Technology, Moscow 141700, Russia.
§Also at the Functional Electronics Laboratory, Tomsk State University, Tomsk, 634050, Russia.
‖Also at Istanbul Arel University, 34295 Istanbul, Turkey.
¶Also at University of Texas at Dallas, Richardson, Texas 75083, USA.
**Also at the NRC "Kurchatov Institute", PNPI, 188300, Gatchina, Russia.
††Also at Bogazici University, 34342 Istanbul, Turkey.

MDC and flight time in TOF is used to form particle identification confidence levels for the π, K and p hypotheses. Each track is assigned the particle type corresponding to the highest confidence level. Photon candidates are required to have an energy deposition above 25 MeV in the barrel EMC ($|\cos\theta| < 0.80$) and 50 MeV in the end cap EMC ($0.86 < |\cos\theta| < 0.92$). To exclude showers from charged particles, the angle between the shower position and the charged tracks extrapolated to the EMC must be greater than 10 degrees. A requirement on the EMC timing is used to suppress electronic noise and energy deposits unrelated to the event.

The study of the $\gamma K^+K^-K^+K^-$ final state is complicated by low momentum kaons significantly affecting the reconstruction efficiency, especially at low $\phi\phi$ masses. To improve the reconstruction efficiency, the $J/\psi \to \gamma K^+K^-K^+K^-$ candidate decays are reconstructed with at least one photon and at least three charged tracks identified as kaons. A one-constraint (1C) kinematic fit under the hypothesis $J/\psi \to \gamma K^+K^-K^\pm K^\mp_{\rm miss}$ is performed by constraining the mass of the missing particle to the kaon mass. The resulting χ^2_{1C} is required to be less than 5. If more than one combination of one photon and three kaon tracks meets this requirement, only the combination with the smallest χ^2_{1C} is accepted. To suppress possible background events with $K^+K^-K^+K^-$ and $\pi^0K^+K^-K^+K^-$ final states, the χ^2 of a 1C kinematic fit under the hypothesis $J/\psi \to K^+K^-K^\pm K^\mp_{\rm miss}$ and the χ^2 of a 2C kinematic fit under the hypothesis $J/\psi \to \pi^0K^+K^-K^\pm K^\mp_{\rm miss}$, with an additional constraint on the invariant mass of the two photons to be equal to the π^0 mass, are both required to be larger than 10.

For the selected $J/\psi \to \gamma K^+K^-K^\pm K^\mp_{\rm miss}$ candidates, one ϕ is reconstructed from the K^+K^- pair with an invariant mass closest to the nominal pole mass m_ϕ, and the other ϕ is reconstructed from the remaining reconstructed kaon and the missing kaon. The scatter plot of $M(K^+K^-)$ versus $M(K^\pm K^\mp_{\rm miss})$ is shown in Fig. 1(a), where a cluster of events corresponding to $\phi\phi$ production is evident. Because the processes $J/\psi \to \phi\phi$ and $J/\psi \to \pi^0\phi\phi$ are forbidden by C-parity conservation, the presence of two ϕ mesons is a clear signal for the radiative decay $J/\psi \to \gamma\phi\phi$. The $\phi\phi$ events are selected by requiring $|M(K^+K^-) - m_\phi| < 10\ {\rm MeV}/c^2$ (referred to as ϕ_1) and $|M(K^\pm K^\mp_{\rm miss}) - m_\phi| < 15\ {\rm MeV}/c^2$ (referred to as ϕ_2). Simulation studies show that only 0.2% of the selected $J/\psi \to \gamma\phi\phi$ events have a miscombination of kaons. The Dalitz plot and the invariant mass distributions of $\phi\phi$ for the selected $\gamma\phi\phi$ candidate events are shown in Figs. 1(b) and 1(c), respectively. A total

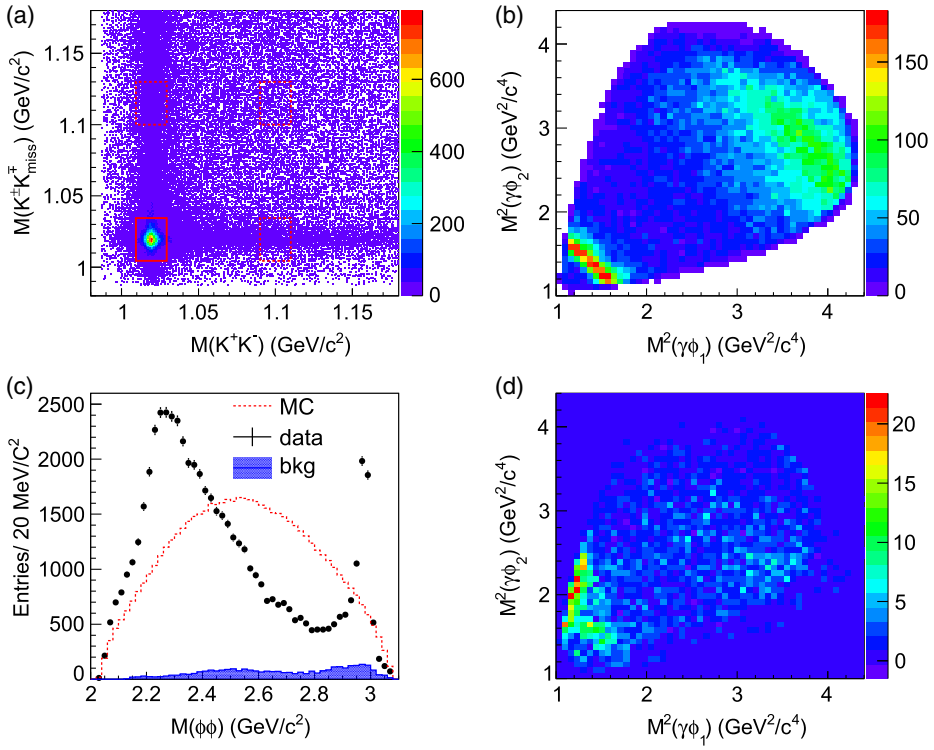

FIG. 1. (a) Scatter plot of $M(K^+K^-)$ versus $M(K^\pm K^\mp_{\rm miss})$ for the selected $\gamma K^+K^-K^\pm K^\mp_{\rm miss}$ candidates. The solid box and dashed boxes show the signal and sideband regions as defined in the text, respectively. (b) The corresponding Dalitz plot for the selected $\gamma\phi\phi$ candidates. (c) Invariant mass distributions of $\phi\phi$ for the selected $\gamma\phi\phi$ candidates. The points with error bars and the dashed line show data and simulation, respectively; the shaded histogram shows the background estimated from $\phi\phi$ sidebands. (d) The corresponding Dalitz plot for the background events estimated from $\phi\phi$ sidebands.

of 58,049 events survive the event selection criteria. Besides a distinct η_c signal, clear structures in the $\phi\phi$ invariant mass spectrum are observed.

Possible backgrounds are studied with a MC sample of 1.2×10^9 J/ψ inclusive decays, in which the decays with known branching fractions are generated by EVTGEN [20] and the remaining J/ψ decays are generated according to the LUNDCHARM [21,22] model. The dominant backgrounds are found to be those with final states $\pi^0K^+K^-K^+K^-$, $K^+K^-K^\pm\pi^\mp K_L$ and $\pi^0\pi^0K^+K^-K^\pm\pi^\mp$, such as $J/\psi\to\phi f_1(1420)$, $f_1(1420)\to K\bar{K}\pi$ and $J/\psi\to\phi K^{*\pm}K^\mp$. No background event with $\phi\phi$ in the final state is observed.

Non-$\phi\phi$ backgrounds are estimated using the ϕ sideband events from data. The two dimensional sidebands are illustrated by dashed boxes in Fig. 1(a), where the sideband regions are defined as $1.09\ \mathrm{GeV}/c^2 < M(K^+K^-) < 1.11\ \mathrm{GeV}/c^2$ and $1.10\ \mathrm{GeV}/c^2 < M(K^\pm K^\mp_{\mathrm{miss}}) < 1.13\ \mathrm{GeV}/c^2$. The shaded histogram in Fig. 1(c) shows the background contribution estimated from the normalized sideband events, corresponding to a background level of 5.4%. The Dalitz plot for the estimated background events are shown in Fig. 1(d), where the accumulation of events in the left lower corner is mainly due to background events from $J/\psi\to\phi f_1(1420)$.

IV. PARTIAL WAVE ANALYSIS

A. Analysis method

Using the GPUPWA framework [23], a PWA is performed on 45 852 events in the region $M(\phi\phi)<2.7\mathrm{GeV}/c^2$ in order to disentangle the structures present in the light mesons. Due to the detector resolution not being included in the PWA fit, events in the η_c signal region are excluded. The quasi two-body decay amplitudes in the sequential decay process $J/\psi\to\gamma X$, $X\to\phi\phi$, $\phi\to K^+K^-$ are constructed using the covariant tensor amplitudes described in Ref. [24]. $J/\psi\to\phi f_1(1285)$, $f_1(1285)\to\gamma\phi$ is ignored due to its low branching fraction [25]. For the radiative J/ψ decay to mesons, the general form for the decay amplitude is

$$A=\psi_\mu(m_1)e^*_\nu(m_2)A^{\mu\nu}=\psi_\mu(m_1)e^*_\nu(m_2)\Sigma_i\Lambda_iU_i^{\mu\nu},\quad(1)$$

where $\psi_\mu(m_1)$ is the J/ψ polarization four-vector, $e_\nu(m_2)$ is the polarization vector of the photon and $U_i^{\mu\nu}$ is the partial wave amplitude with coupling strength determined by a complex parameter Λ_i. The partial wave amplitudes U_i used in the analysis are constructed with the four-momenta of the particles in the final state, and their specific expressions are given in Ref. [24].

In this analysis, we use Breit-Wigner (BW) as an approximation to describe the leading singularity since no model is available yet for the high energy region with many channels opened. Each resonance X is parametrized by a constant-width, relativistic BW propagator,

$$BW(s)=\frac{1}{M^2-s-iM\Gamma},\quad(2)$$

where s is the invariant mass-squared of $\phi\phi$, and M and Γ are the mass and width of the intermediate resonance.

The complex coefficients of the amplitudes and resonance parameters are determined by an unbinned maximum likelihood fit with the likelihood function constructed as in Ref. [26].

The probability to observe the ith event characterized by the measurement ξ_i, i.e., the measured four-momenta of the particles in the final state, is:

$$P(\xi_i)=\frac{\omega(\xi_i)\epsilon(\xi_i)}{\int d\xi\omega(\xi)\epsilon(\xi)},\quad(3)$$

where $\epsilon(\xi_i)$ is the detection efficiency and $\omega(\xi_i)\equiv(\frac{d\sigma}{d\Phi})_i$ is the differential cross section, and $d\Phi$ is the standard element of phase space. The full differential cross section is:

$$\frac{d\sigma}{d\Phi}=\left|\sum A(J^{PC})\right|^2,\quad(4)$$

where $A(J^{PC})$ is the full amplitude for all possible resonances whose spin-parity are J^{PC}. $\int d\xi\omega(\xi)\epsilon(\xi)\equiv\sigma'$ is the measured total cross section.

The joint probability density for observing the N events in the data sample is:

$$\mathcal{L}=\prod_{i=1}^{N}P(\xi_i)=\prod_{i=1}^{N}\frac{(\frac{d\sigma}{d\Phi})_i\epsilon(\xi_i)}{\sigma'}.\quad(5)$$

For technical reasons, rather than maximizing $\mathcal{L}$, $\mathcal{S}=-\ln\mathcal{L}$ is minimized, with

$$\mathcal{S}=-\ln\mathcal{L}=-\sum_{i=1}^{N}\ln\left(\frac{(\frac{d\sigma}{d\Phi})_i}{\sigma'}\right)-\sum_{i=1}^{N}\ln\epsilon(\xi_i),\quad(6)$$

for a given data set. The second term is a constant and has no impact on the determination of the parameters of the amplitudes or on the relative changes of $\mathcal{S}$ values. In the fitting, $-\ln\mathcal{L}$ is defined as:

$$-\ln\mathcal{L}=-\sum_{i=1}^{N}\ln\left(\frac{(\frac{d\sigma}{d\Phi})_i}{\sigma'}\right)=-\sum_{i=1}^{N}\ln\left(\frac{d\sigma}{d\Phi}\right)_i+N\ln\sigma'.\quad(7)$$

The free parameters are optimized by MINUIT [27]. The measured total cross section σ' is evaluated using MC techniques. An MC sample of N_{gen} is generated with signal events that are distributed uniformly in phase space. These events are subjected to the selection criteria and yield a

sample of $N_{\rm acc}$ accepted events. The normalization integral is computed as:

$$\int d\xi\omega(\xi)\epsilon(\xi) = \sigma' \to \frac{1}{N_{\rm acc}}\sum_{k}^{N_{\rm acc}}\left(\frac{d\sigma}{d\Phi}\right)_k. \quad (8)$$

Since data contains the contribution of signal and background, the contribution of non-$\phi\phi$ background events is taken into account by subtracting the negative log-likelihood (NLL) value obtained for events in the $\phi\phi$ sidebands from the NLL value obtained for events in the $\phi\phi$ signal region, i.e.,

$$\mathcal{L}_{\rm sig} = \frac{\mathcal{L}_{\rm data}}{\mathcal{L}_{\rm bkg}}, \quad (9)$$

$$-\ln\mathcal{L}_{\rm sig} = -(\ln\mathcal{L}_{\rm data} - \ln\mathcal{L}_{\rm bkg}). \quad (10)$$

The number of the fitted events N_X for an intermediate resonance X, which has N_{W_X} independent partial wave amplitudes A_i, is defined as

$$N_X = \frac{\sigma_X}{\sigma'}\cdot N', \quad (11)$$

where N' is the number of selected events after background subtraction, and

$$\sigma_X = \frac{1}{N_{\rm acc}}\sum_{k}^{N_{\rm acc}}\left|\sum_{j}^{N_{W_X}}(A_j)_k\right|^2 \quad (12)$$

is the measured cross section of the resonance X and is calculated with the same MC sample as the measured total cross section σ'.

The branching fraction of $J/\psi \to \gamma X, X \to \phi\phi$ is calculated as:

$$\mathcal{B}(J/\psi \to \gamma X \to \gamma\phi\phi) = \frac{N_X}{N_{J/\psi}\cdot\varepsilon_X\cdot\mathcal{B}^2_{\phi\to K^+K^-}}, \quad (13)$$

where the detection efficiency ε_X is obtained by the partial wave amplitude weighted MC sample,

$$\varepsilon_X = \frac{\sigma_X}{\sigma_X^{\rm gen}} = \frac{\sum_k^{N_{\rm acc}}|\sum_j^{N_{W_X}}(A_j)_k|^2}{\sum_i^{N_{\rm gen}}|\sum_j^{N_{W_X}}(A_j)_i|^2}, \quad (14)$$

$N_{J/\psi}$ is the total number of J/ψ events, and $\mathcal{B}_{\phi\to K^+K^-} = (48.9\pm0.5)\%$ is the branching fraction of $\phi \to K^+K^-$ taken from Ref. [25].

B. PWA results

In this analysis, all possible combinations of $J^{PC} = 0^{-+}$, 0^{++} and 2^{++} resonances [28] listed in the PDG [25] are evaluated. Given the small phase space of $J/\psi \to \gamma\phi\phi$, $J \geq 4$ states should be suppressed. The changes in the NLL value and the number of free parameters in the fit with and without a resonance are used to evaluate its statistical significance. In the baseline solution, there are three 0^{-+} resonances ($\eta(2225)$, $\eta(2100)$, and $X(2500)$), one 0^{++} resonance ($f_0(2100)$), three 2^{++} resonances ($f_2(2010)$, $f_2(2300)$, and $f_2(2340)$), and the direct decay of $J/\psi \to \gamma\phi\phi$, which is modeled by a 0^{-+} phase space distribution (0^{-+} PHSP) of the $\phi\phi$ system. The statistical significance of each component in the baseline solution is larger than 5σ. The masses and widths of the three 0^{-+} resonances are free parameters in the fit. The resonance parameters of the 0^{++} and 2^{++} resonances are fixed to the PDG [25] values due to limited statistics. The masses and widths of the resonances, product branching fractions of $J/\psi \to \gamma X$, $X \to \phi\phi$, and the statistical significances are summarized in Table I, where the first errors are statistical, and the second ones are systematic. The fit fraction of each component and their interference fractions are shown in Table II. Figure 2(a) shows a comparison of the data and the PWA fit projection (weighted by MC efficiencies) of the invariant mass distributions of $\phi\phi$ for the fitted parameters. The comparisons of the projected data and MC angular distributions for the events with $\phi\phi$ invariant mass less than 2.7 GeV/c^2 are shown in Fig. 2(b)–2(e). The $\chi^2/n_{\rm bin}$ value is displayed on each figure to demonstrate the goodness of fit, where $n_{\rm bin}$ is the number of bins of each figure and χ^2 is defined as:

$$\chi^2 = \sum_{i=1}^{n_{\rm bin}}\frac{(n_i-\nu_i)^2}{\nu_i}, \quad (15)$$

where n_i and ν_i are the number of events for the data and the fit projections with the baseline solution in the ith bin of each figure, respectively.

TABLE I. Mass, width, $\mathcal{B}(J/\psi \to \gamma X \to \gamma\phi\phi)$ (B.F.) and significance (Sig.) of each component in the baseline solution. The first errors are statistical and the second ones are systematic.

Resonance	M (MeV/c^2)	Γ (MeV/c^2)	B.F. ($\times10^{-4}$)	Sig.
$\eta(2225)$	2216^{+4+21}_{-5-11}	185^{+12+43}_{-14-17}	$(2.40\pm0.10^{+2.47}_{-0.18})$	28σ
$\eta(2100)$	2050^{+30+75}_{-24-26}	$250^{+36+181}_{-30-164}$	$(3.30\pm0.09^{+0.18}_{-3.04})$	22σ
$X(2500)$	$2470^{+15+101}_{-19-23}$	230^{+64+56}_{-35-33}	$(0.17\pm0.02^{+0.02}_{-0.08})$	8.8σ
$f_0(2100)$	2101	224	$(0.43\pm0.04^{+0.24}_{-0.03})$	24σ
$f_2(2010)$	2011	202	$(0.35\pm0.05^{+0.28}_{-0.15})$	9.5σ
$f_2(2300)$	2297	149	$(0.44\pm0.07^{+0.09}_{-0.15})$	6.4σ
$f_2(2340)$	2339	319	$(1.91\pm0.14^{+0.72}_{-0.73})$	11σ
0^{-+} PHSP			$(2.74\pm0.15^{+0.16}_{-1.48})$	6.8σ

Various checks are performed to test the reliability of the model-dependent PWA solution. Replacing the pseudoscalar state $\eta(2100)$ by either $\eta(2010)$ [29] or $\eta(2320)$ [30]

TABLE II. Fraction of each component and interference fractions between two components (%) in the baseline solution. The errors are statistical only.

Resonance	$\eta(2100)$	$\eta(2225)$	$X(2500)$	0^{-+} PHSP	$f_0(2100)$	$f_2(2010)$	$f_2(2300)$	$f_2(2340)$
$\eta(2100)$	54.2 ± 1.5	43.5 ± 1.2	15.2 ± 1.0	-64.0 ± 2.2	0.0 ± 0.0	0.0 ± 0.0	0.0 ± 0.0	-0.1 ± 0.0
$\eta(2225)$		41.0 ± 1.6	15.9 ± 0.7	-60.6 ± 1.7	0.0 ± 0.0	0.0 ± 0.0	0.1 ± 0.0	-0.1 ± 0.0
$X(2500)$			3.2 ± 0.3	-15.7 ± 1.0	0.0 ± 0.0	0.0 ± 0.0	0.0 ± 0.0	0.0 ± 0.0
0^{-+} PHSP				42.8 ± 2.3	0.0 ± 0.0	0.0 ± 0.0	0.0 ± 0.0	0.0 ± 0.0
$f_0(2100)$					6.5 ± 0.6	0.1 ± 0.0	0.1 ± 0.0	-0.5 ± 0.0
$f_2(2010)$						5.9 ± 0.8	6.0 ± 0.7	-18.6 ± 1.6
$f_2(2300)$							8.8 ± 1.4	-22.0 ± 3.5
$f_2(2340)$								38.4 ± 2.8

worsens the NLL values by 21.2 and 33.0, respectively. The spin-parity assignment J^{PC} of the $X(2500)$ as 0^{-+} is significantly better than the 0^{++} hypothesis, with the NLL value improving by 44.1 units. Changing the spin-parity assignment of the $X(2500)$ to 2^{++}, resulting in 10 additional free parameters, worsens the NLL value by 0.5, instead. Therefore, the preferred assignment for the $X(2500)$ is pseudoscalar. If we replace the two tensor states $f_2(2300)$ and $f_2(2340)$ by a single one with free resonance parameters in the fit, the NLL value is worsened by 14.7. In this case, a statistical significance test of the $f_2(2340)$ yields a value of 6.1σ. The narrow $f_J(2220)$ (alternatively known as the $\xi(2230)$), which was seen in $J/\psi \to \gamma K^+K^-$ at MarkIII [31] and BES [32], but not seen in $J/\psi \to \gamma K^0_S K^0_S$ at CLEO [33], is also studied. When included in the PWA, the statistical significance of the $f_J(2220)$ is found to be 0.8σ. The upper limit on the branching fraction ratio $\mathcal{B}(\xi(2230) \to \phi\phi)/\mathcal{B}(\xi(2230) \to K^+K^-)$ at the 90% C.L. is estimated to be 1.91×10^{-2}. For the description of the nonresonant contribution, the statistical significance of additional non-resonant contributions with $J^{PC} = 0^{++}$ or 2^{++} is less than 5σ. Additional

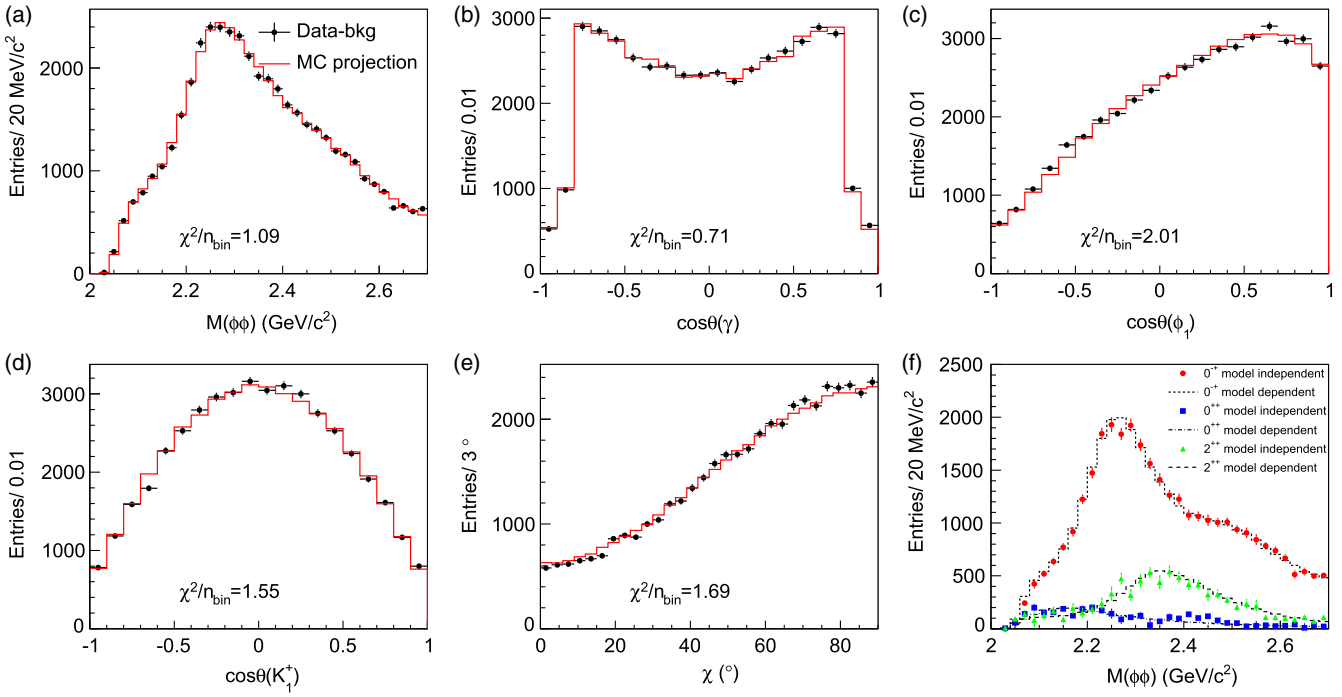

FIG. 2. Superposition of data and the PWA fit projections for: (a) invariant mass distributions of $\phi\phi$; (b) $\cos\theta$ of γ in the J/ψ rest frame; (c) $\cos\theta$ of ϕ_1 in the X rest frame; (d) $\cos\theta$ of K^+ in the ϕ_1 rest frame; (e) the azimuthal angle between the normals to the two decay planes of ϕ in the X rest frame. Black dots with error bars are data with background events subtracted and the solid red lines are projections of the model-dependent fit. (f) Intensities of individual J^{PC} components. The red dots, blue boxes and green triangles with error bars are the intensities of $J^{PC} = 0^{-+}$, 0^{++} and 2^{++}, respectively, from the model-independent fit in each bin. The short-dashed, dash-dotted and long-dashed histograms show the coherent superpositions of the BW resonances with $J^{PC} = 0^{-+}$, 0^{++} and 2^{++}, respectively, from the model-dependent fit.

TABLE III. Additional resonances, J^{PC}, change of number of free parameters (ΔNdof), change of NLL (ΔNLL) and corresponding significance (Sig.).

Resonance	J^{PC}	ΔNdof	ΔNLL	Sig.
$f_0(2020)$	0^{++}	4	11.5	3.8σ
$f_0(2330)$	0^{++}	4	4.3	1.8σ
$f_0(2200)$	0^{++}	4	5.0	2.0σ
$f_2(2150)$	2^{++}	12	25.1	4.8σ
$f_J(2220)$	2^{++}	12	6.3	0.8σ
$\eta(2010)$	0^{-+}	2	1.5	1.2σ
$\eta(2320)$	0^{-+}	2	0.4	0.4σ
	0^{-+}	2	0.5	0.5σ
$X(2370)$	0^{++}	4	5.4	2.2σ
	2^{++}	12	17.8	3.5σ
	0^{-+}	2	1.3	1.1σ
$X(2120)$	0^{++}	4	2.3	0.9σ
	2^{++}	12	14.9	3.0σ

resonances listed in Ref. [25] as well as two extra states, the $X(2120)$ and $X(2370)$ from Ref. [34], are tested with all possible J^{PC} assignments. None of them has a statistical significance larger than 5σ, as shown in Table III. The existence of possible additional resonances is further studied by performing scans for extra resonances ($J^{PC} = 0^{-+}$, 0^{++}, 1^{++}, 2^{-+}, 2^{++} and 4^{++}) with different masses and widths. The scan results yield no evidence for extra intermediate states. The reliability of the fit procedure is tested by an input-output check, as follows: An MC sample is generated with given components. After the fitting procedure described above, the properties of the components (mass, width, branching fraction, and the effect of interference terms) are compared with the input values. The output values agree with the input around $\pm 1\sigma$, confirming the reliability of the fitting procedure.

In addition to the PWA fit with resonances described by BW functions, a model-independent fit where the intermediate states are parametrized by a separate complex constant for each of 35 bins of 20 MeV/c^2 width is performed in the region $M(\phi\phi) < 2.7$ GeV/c^2 to extract the contribution of components with each J^{PC} using the method described in Ref. [35]. The fit results are shown in Fig. 2(f). The 0^{-+} contribution is dominant, and a strong 2^{++} component at 2.3 GeV/c^2 is observed. In general, the model-independent fit gives similar features to those of the model-dependent fit, and the results of these two fits are consistent with each other.

V. SYSTEMATIC UNCERTAINTIES

The sources of systematic uncertainty are divided into two categories. The first includes the systematic uncertainties from the number of J/ψ events (0.8% [36,37]), MDC tracking (1.0% each for three charged tracks [38]), kaon PID (1.0% each for three kaons [38]), photon detection efficiency (1.0% [38]), kinematic fit (2.5%), ϕ mass resolution (0.3%) and $\mathcal{B}_{\phi\to K^+K^-}$ (2.0%). These systematic uncertainties are applicable to all the branching fraction measurements. The total systematic uncertainty from these sources is 5.5%. The second source concerns the PWA fit procedure, where the systematic uncertainties are applicable to measurements of the branching fractions and resonance parameters. These sources of systematic uncertainties are described below.

(i) BW parametrization. Uncertainties from the BW parametrization are estimated by the changes in the fit results caused by replacing the fixed width Γ_0 of the BW for the threshold states $\eta(2100)$ and $\eta(2225)$ with a mass-dependent width form $\Gamma(m)$ [39].

(ii) Uncertainty from resonance parameters. In the nominal fit, the resonance parameters of the 0^{++} and 2^{++} states are fixed. An alternative fit is performed in which those resonance parameters are varied within one standard deviation of the PDG values [25], and the changes in the results are taken as systematic uncertainties.

(iii) Background uncertainty. To estimate the background uncertainty, alternative fits are performed with background events from different ϕ sideband regions and different normalization factors, and the

TABLE IV. Summary of the systematic error sources and their corresponding contributions (in MeV/c^2) to the systematic uncertainties in masses and widths of $\eta(2100)$, $\eta(2225)$ and $X(2500)$, denoted as ΔM and ΔΓ, respectively.

		$\eta(2100)$		$\eta(2225)$		$X(2500)$	
Sources		ΔM	ΔΓ	ΔM	ΔΓ	ΔM	ΔΓ
Breit-Wigner parametrization		$^{+72}_{-10}$	$^{+164}_{-152}$	$^{+9}_{-10}$	$^{+43}_{-0}$	$^{+20}_{-5}$	$^{+15}_{-30}$
Resonance parameters		$^{+1}_{-0}$	$^{+1}_{-0}$	$^{+0}_{-1}$	$^{+0}_{-1}$	$^{+0}_{-2}$	$^{+0}_{-3}$
Background uncertainty		$^{+20}_{-22}$	$^{+64}_{-10}$	$^{+11}_{-5}$	$^{+6}_{-5}$	$^{+42}_{-20}$	$^{+36}_{-10}$
Extra resonances	$f_2(2150)$	$^{+0}_{-10}$	$^{+40}_{-0}$	$^{+10}_{-0}$	$^{+0}_{-6}$	$^{+0}_{-10}$	$^{+0}_{-10}$
	Other insignificant resonances	$^{+10}_{-0}$	$^{+0}_{-60}$	$^{+12}_{-0}$	$^{+0}_{-15}$	$^{+90}_{-0}$	$^{+40}_{-0}$
Total		$^{+75}_{-26}$	$^{+181}_{-164}$	$^{+21}_{-11}$	$^{+43}_{-17}$	$^{+101}_{-23}$	$^{+56}_{-33}$

TABLE V. Summary of the systematic error sources and their corresponding contributions to the branching fractions of $J/\psi \to \gamma X \to \gamma\phi\phi$ (relative uncertainties, in %), which are denoted as $\Delta\mathcal{B}$.

Sources		$\eta(2100)$	$\eta(2225)$	$X(2500)$	$f_0(2100)$	$f_2(2010)$	$f_2(2300)$	$f_2(2340)$	0^{-+} PHSP
Event selection		±5.5	±5.5	±5.5	±5.5	±5.5	±5.5	±5.5	±5.5
Breit-Wigner parametrization		$^{+0.0}_{-91.8}$	$^{+102.9}_{-0.0}$	$^{+0.0}_{-48.0}$	$^{+0.4}_{-2.1}$	$^{+23.7}_{-0.0}$	$^{+7.9}_{-0.6}$	$^{+0.0}_{-12.3}$	$^{+0.0}_{-53.4}$
Resonance parameters		$^{+0.0}_{-2.7}$	$^{+0.0}_{-3.7}$	$^{+0.0}_{-11.8}$	$^{+0.9}_{-0.0}$	$^{+0.0}_{-11.9}$	$^{+15.7}_{-0.0}$	$^{+0.0}_{-13.7}$	$^{+0.0}_{-5.8}$
Background uncertainty		$^{+0.7}_{-0.2}$	$^{+0.9}_{-0.1}$	$^{+10.4}_{-0.1}$	$^{+1.8}_{-0.1}$	$^{+1.6}_{-3.1}$	$^{+7.4}_{-3.3}$	$^{+1.2}_{-0.7}$	$^{+1.7}_{-0.2}$
Extra resonances	$f_2(2150)$	$^{+0.0}_{-3.1}$	$^{+0.0}_{-3.4}$	$^{+0.0}_{-4.5}$	$^{+0.0}_{-0.1}$	$^{+75.6}_{-0.0}$	$^{+0.0}_{-18.1}$	$^{+37.3}_{-0.0}$	$^{+0.0}_{-3.0}$
	Other insignificant resonances	$^{+0.0}_{-0.6}$	$^{+0.0}_{-2.0}$	$^{+0.0}_{-0.8}$	$^{+56.6}_{-0.0}$	$^{+0.0}_{-41.3}$	$^{+0.0}_{-28.1}$	$^{+0.0}_{-32.8}$	$^{+0.0}_{-2.8}$
Total		$^{+5.5}_{-92.1}$	$^{+103.1}_{-7.7}$	$^{+11.8}_{-49.9}$	$^{+56.9}_{-5.9}$	$^{+79.4}_{-43.4}$	$^{+19.8}_{-34.0}$	$^{+37.7}_{-38.0}$	$^{+5.8}_{-54.2}$

changes in the results are assigned as the systematic uncertainties.

(iv) Uncertainty from additional resonances. Uncertainties from possible additional resonances are estimated by adding the $f_0(2020)$ and the $f_2(2150)$, which are the two most significant additional resonances, into the baseline configuration individually, the changes of the measurements caused by them are assigned as the systematic uncertainties.

For each alternative fit performed to estimate the systematic uncertainties from the PWA fit procedure, the changes of the measurements are taken as the one-sided systematic uncertainties. For each measurement, the individual uncertainties are assumed to be independent and are added in quadrature to obtain the total systematic uncertainty on the negative and positive side, respectively. The sources of systematic uncertainties applicable to the measurements of masses and widths of $\eta(2225)$, $\eta(2100)$ and $X(2500)$, and their contributions are summarized in Table IV. The relative systematic uncertainties relevant for the branching fraction measurements are summarized in Table V, where the last row is the total relative systematic uncertainty from fitting irrelevant sources.

VI. SUMMARY

In summary, a PWA on $J/\psi \to \gamma\phi\phi$ has been performed based on $(1310.6 \pm 10.5) \times 10^6$ J/ψ events collected with the BESIII detector. The most remarkable feature of the PWA results is that 0^{-+} states are dominant. The existence of the $\eta(2225)$ is confirmed and two additional pseudoscalar states, $\eta(2100)$ with a mass 2050^{+30+75}_{-24-26} MeV/c^2 and a width $250^{+36+181}_{-30-164}$ MeV/c^2 and $X(2500)$ with a mass $2470^{+15+101}_{-19-23}$ MeV/c^2 and a width 230^{+64+56}_{-35-33} MeV/c^2, are observed. The new experimental results are helpful for mapping out pseudoscalar excitations and searching for a 0^{-+} glueball. The three tensors $f_2(2010)$, $f_2(2300)$ and $f_2(2340)$ observed in $\pi^- p \to \phi\phi n$ [9] are also observed in $J/\psi \to \gamma\phi\phi$. Recently, the production rate of the pure gauge tensor glueball in J/ψ radiative decays has been predicted by Lattice QCD [40], which is compatible with the large production rate of the $f_2(2340)$ in $J/\psi \to \gamma\phi\phi$ and $J/\psi \to \gamma\eta\eta$ [26].

ACKNOWLEDGMENTS

The BESIII Collaboration thanks the staff of BEPCII and the IHEP computing center for their strong support. This work is supported in part by the National Key Basic Research Program of China under Contract No. 2015CB856700; National Natural Science Foundation of China (NSFC) under Contracts No. 11235011, No. 11322544, No. 11335008, No. 11425524; the Chinese Academy of Sciences (CAS) Large-Scale Scientific Facility Program; the CAS Center for Excellence in Particle Physics (CCEPP); the Collaborative Innovation Center for Particles and Interactions (CICPI); Joint Large-Scale Scientific Facility Funds of the NSFC and CAS under Contracts No. U1232201, No. U1332201; CAS under Contracts No. KJCX2-YW-N29, No. KJCX2-YW-N45; 100 Talents Program of CAS; National 1000 Talents Program of China; INPAC and Shanghai Key Laboratory for Particle Physics and Cosmology; Istituto Nazionale di Fisica Nucleare, Italy; Joint Large-Scale Scientific Facility Funds of the NSFC and CAS under Contract No. U1532257; Joint Large-Scale Scientific Facility Funds of the NSFC and CAS under Contract No. U1532258; Koninklijke Nederlandse Akademie van Wetenschappen (KNAW) under Contract No. 530-4CDP03; Ministry of Development of Turkey under Contract No. DPT2006K-120470; The Swedish Resarch Council; U.S. Department of Energy under Contracts No. DE-FG02-05ER41374, No. DE-SC-0010504, No. DE-SC0012069, No. DESC0010118; U.S. National Science Foundation; University of Groningen (RuG) and the Helmholtzzentrum fuer Schwerionenforschung GmbH (GSI), Darmstadt; WCU Program of National Research Foundation of Korea under Contract No. R32-2008-000-10155-0.

[1] C. Amsler and N. A. Tornqvist, Phys. Rep. **389**, 61 (2004).
[2] E. Klempt and A. Zaitsev, Phys. Rep. **454**, 1 (2007).
[3] V. Crede and C. A. Meyer, Prog. Part. Nucl. Phys. **63**, 74 (2009).
[4] G. S. Bali, K. Schilling, A. Hulsebos, A. C. Irving, C. Michael, and P. W. Stephenson (UKQCD Collaboration), Phys. Lett. B **309**, 378 (1993).
[5] C. J. Morningstar and M. Peardon, Phys. Rev. D **60**, 034509 (1999).
[6] Y. Chen *et al.*, Phys. Rev. D **73**, 014516 (2006).
[7] M. B. Cakir and G. R. Farrar, Phys. Rev. D **50**, 3268 (1994).
[8] F. E. Close, G. R. Farrar, and Z. P. Li, Phys. Rev. D **55**, 5749 (1997).
[9] A. Etkin *et al.*, Phys. Rev. Lett. **41**, 784 (1978); Phys. Lett. **165B**, 217 (1985); **201**, 568 (1988).
[10] P. S. L. Booth *et al.*, Nucl. Phys. **B273**, 677 (1986).
[11] D. Barberis *et al.*, Phys. Lett. B **432**, 436 (1998).
[12] C. Evangelista *et al.* (JETSET Collaboration), Phys. Rev. D **57**, 5370 (1998).
[13] S. J. Lindenbaum and R. S. Longacre, Phys. Lett. **165B**, 202 (1985).
[14] R. S. Longacre and S. J. Lindenbaum, Phys. Rev. D **70**, 094041 (2004).
[15] D. Bisello *et al.* (DM2 Collaboration), Phys. Lett. B **179**, 294 (1986); **241**, 617 (1990).
[16] Z. Bai *et al.* (MARKIII Collaboration), Phys. Rev. Lett. **65**, 1309 (1990).
[17] J. Z. Bai *et al.* (BESII Collaboration), Phys. Lett. B **662**, 330 (2008).
[18] M. Ablikim *et al.* (BESIII Collaboration), Nucl. Instrum. Methods Phys. Res., Sect. A **614**, 345 (2010).
[19] S. Agostinelli *et al.* (GEANT4 Collaboration), Nucl. Instrum. Methods Phys. Res., Sect. A **506**, 250 (2003).
[20] D. J. Lange, Nucl. Instrum. Methods Phys. Res., Sect. A **462**, 152 (2001).
[21] R. G. Ping, Chin. Phys. C **32**, 599 (2008).
[22] R. L. Yang, R. G. Ping, and H. Chen, Chin. Phys. Lett. **31**, 061301 (2014).
[23] N. Berger, B. J. Liu, and J. K. Wang, J. Phys. Conf. Ser. **219**, 042031 (2010).
[24] B. S. Zou and D. V. Bugg, Eur. Phys. J. A **16**, 537 (2003).
[25] K. A. Olive *et al.* (Particle Data Group Collaboration), Chin. Phys. C **38**, 090001 (2014).
[26] M. Ablikim *et al.* (BESIII Collaboration), Phys. Rev. D **87**, 092009 (2013).
[27] F. James and M. Roos, Comput. Phys. Commun. **10**, 343 (1975).
[28] We tested the following mesons listed in PDG 2014 (those with a * are from the Further States table): $\eta(2010)^*$, $f_2(2010)$, $f_0(2020)$, $\eta(2100)^*$, $f_0(2100)$, $f_2(2150)$, $f_0(2200)$, $f_J(2220)$, $\eta(2225)$, $f_2(2300)$, $\eta(2320)^*$, $f_0(2330)$, $f_2(2340)$.
[29] A. V. Anisovich, C. A. Baker, C. J. Batty, D. V. Bugg, C. Hodd, H. C. Lu, V. A. Nikonov, A. V. Sarantsev, V. V. Sarantsev, and B. S. Zou, Phys. Lett. B **491**, 47 (2000).
[30] A. V. Anisovich, C. A. Baker, C. J. Batty, D. V. Bugg, V. A. Nikonov, A. V. Sarantsev, V. V. Sarantsev, and B. S. Zou, Phys. Lett. B **496**, 145 (2000).
[31] R. M. Baltrusaitis *et al.*, Phys. Rev. Lett. **56**, 107 (1986).
[32] J. Z. Bai *et al.* (BES Collaboration), Phys. Rev. Lett. **76**, 3502 (1996).
[33] R. Godang *et al.* (CLEO Collaboration), Phys. Rev. Lett. **79**, 3829 (1997).
[34] M. Ablikim *et al.* (BESIII Collaboration), Phys. Rev. Lett. **106**, 072002 (2011).
[35] J. Z. Bai *et al.* (BES Collaboration), Phys. Rev. D **68**, 052003 (2003).
[36] M. Ablikim *et al.* (BESIII Collaboration), Chin. Phys. C **36**, 915 (2012).
[37] With the same approach as in Ref. [36], the preliminary number of J/ψ events taken in 2009 and 2012 is determined to be 1310.6×10^6 with an uncertainty of 0.8%.
[38] M. Ablikim *et al.* (BESIII Collaboration), Phys. Rev. D **83**, 112005 (2011).
[39] J. H. Kühn and A. Santamaria, Z. Phys. C **48**, 445 (1990).
[40] Y.-B. Yang, L.-C. Gui, Y. Chen, C. Liu, Y.-B. Liu, J.-P. Ma, and J.-B. Zhang, Phys. Rev. Lett. **111**, 091601 (2013).